

AD-A065 482

AEROSPACE CORP EL SEGUNDO CALIF IVAN A GETTING LABS

F/6 21/3

MAGNETOSPHERIC AND IONOSPHERIC IMPACT OF LARGE-SCALE SPACE TRAN--ETC(U)

JAN 79 Y T CHIU, J G LUHMANN, B K CHING

F04701-78-C-0079

UNCLASSIFIED

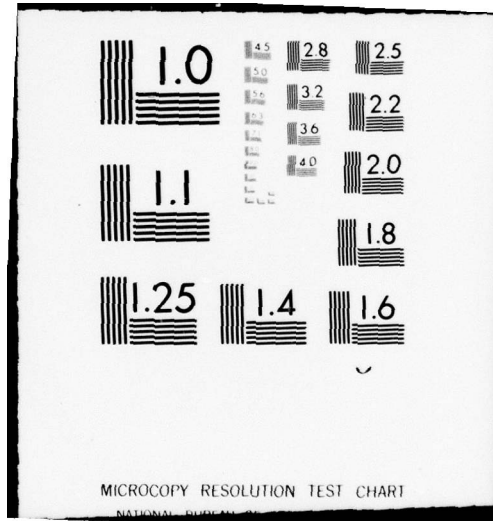
TR-0079(4960-04)-3

SAMSO-TR-79-3

NL

1 OF 1
AD
A065482





LEVEL

12

AD A0 65482

**Magnetospheric and Ionospheric
Impact of Large-Scale
Space Transportation with Ion Engines**

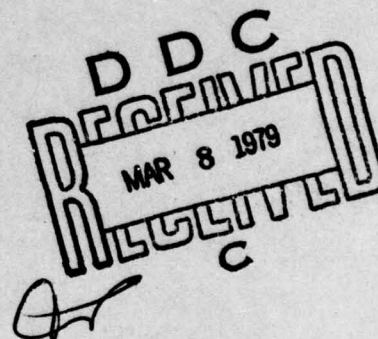
Y. T. CHIU, J. G. LUHMANN, B. K. CHING,
M. SCHULZ, and D. J. BOUCHER, JR.

Space Sciences Laboratory
The Ivan A. Getting Laboratories
The Aerospace Corporation
El Segundo, Calif. 90245

25 January 1979

Interim Report

APPROVED FOR PUBLIC RELEASE;
DISTRIBUTION UNLIMITED



DDC FILE COPY

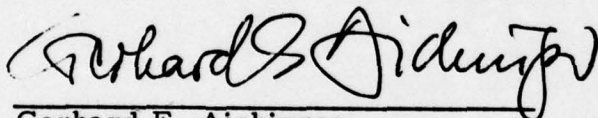
Prepared for
SPACE AND MISSILE SYSTEMS ORGANIZATION
AIR FORCE SYSTEMS COMMAND
Los Angeles Air Force Station
P.O. Box 92960, Worldway Postal Center
Los Angeles, Calif. 90009

79 03 06 037

This interim report was submitted by The Aerospace Corporation, El Segundo, CA 90245, under Contract No. F04701-78-C-0079 with the Space and Missile Systems Organization, Deputy for Advanced Space Programs, P.O. Box 92960, Worldway Postal Center, Los Angeles, CA 90009. It was reviewed and approved for The Aerospace Corporation by G. A. Paulikas, Director, Space Sciences Laboratory. Gerhard E. Aichinger, SAMSO/TM was the project officer for Advanced Space Programs.

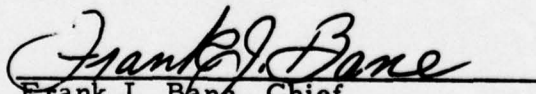
This report has been reviewed by the Information Office (OI) and is releasable to the National Technical Information Service (NTIS). At NTIS, it will be available to the general public, including foreign nations.

This technical report has been reviewed and is approved for publication. Publication of this report does not constitute Air Force approval of the report's findings or conclusions. It is published only for the exchange and stimulation of ideas.



Gerhard E. Aichinger
Project Officer

FOR THE COMMANDER



Frank J. Bane, Chief
Contracts Management Office

UNCLASSIFIED

SECURITY CLASSIFICATION OF THIS PAGE (When Data Entered)

REPORT DOCUMENTATION PAGE		READ INSTRUCTIONS BEFORE COMPLETING FORM
1. REPORT NUMBER	2. GOVT ACCESSION NO.	3. RECIPIENT'S CATALOG NUMBER
18 SAMSO-TR-79-3		
4. TITLE (and Subtitle)		5. TYPE OF REPORT & PERIOD COVERED
6 MAGNETOSPHERIC AND IONOSPHERIC IMPACT OF LARGE-SCALE SPACE TRANSPORTATION WITH ION ENGINES.		Interim rept.
7. AUTHOR(s)		8. PERFORMING ORG. REPORT NUMBER
10 Yam T./Chiu, Janet G./Luhmann, Barbara K./Ching, Michael/Schulz, Donald J./Boucher, Jr.		14 TR-0079(4960-04)-3
9. PERFORMING ORGANIZATION NAME AND ADDRESS		15. CONTRACT OR GRANT NUMBER(s)
The Aerospace Corporation El Segundo, Calif. 90245		15 F04701-78-C-0078
11. CONTROLLING OFFICE NAME AND ADDRESS		10. PROGRAM ELEMENT, PROJECT, TASK AREA & WORK UNIT NUMBERS
Space and Missile Systems Organization Air Force Systems Command Los Angeles, Calif. 90009		12 45R
14. MONITORING AGENCY NAME & ADDRESS (if different from Controlling Office)		12. REPORT DATE
		11 25 Jan 1979
		13. NUMBER OF PAGES
		43
		15. SECURITY CLASS. (of this report)
		Unclassified
		15a. DECLASSIFICATION/DOWNGRADING SCHEDULE
16. DISTRIBUTION STATEMENT (of this Report)		
Approved for public release; distribution unlimited		
17. DISTRIBUTION STATEMENT (of the abstract entered in Block 20, if different from Report)		
18. SUPPLEMENTARY NOTES		
19. KEY WORDS (Continue on reverse side if necessary and identify by block number)		
Environmental Modification Ion Engines Ionosphere Magnetosphere Space Transportation		
20. ABSTRACT (Continue on reverse side if necessary and identify by block number)		
<p>Future large-scale space missions with payloads of $\geq 10^7$ Kg ($\geq 10^4$ tons), such as the proposed Solar Power Satellite and Space Colonization, will probably require deep-space transportation systems based on the high specific-impulse ion engine. We note in this paper that the ion exhaust emissions corresponding to the proposed large payloads required for such missions may introduce basic modifications in the composition and dynamics of the ionosphere and magnetosphere. We identify some effects that such modifications may induce upon</p> <p style="text-align: right;">→ next page</p>		

DD FORM
(FA CSIMILE)

1473

79

03

06

037

409 944

UNCLASSIFIED

SECURITY CLASSIFICATION OF THIS PAGE (When Data Entered)

JOB

UNCLASSIFIED

SECURITY CLASSIFICATION OF THIS PAGE(When Data Entered)

19. KEY WORDS (Continued)

20. ABSTRACT (Continued)

other space systems such as earth sensors, radiation belt dosage environment and signal scintillation due to beam-plasma interactions. We find that, because the space environment is tenuous, there is an interaction of sorts among such large-scale space systems and other earth-oriented space systems. The architectural design of such large-scale systems must take into account not only the efficient functioning of their primary mission objectives but also their influence upon the operations of other space systems.

UNCLASSIFIED

SECURITY CLASSIFICATION OF THIS PAGE(When Data Entered)

CONTENTS

I.	INTRODUCTION	5
II.	ION EXHAUST EMISSION MODEL	9
III.	PLASMASPHERE MODEL WITH ARGORO	21
IV.	ENVIRONMENTAL IMPACT.....	27
	a. Effects on Atmospheric Optical Sensing Systems	27
	b. Ring-Current and Radiation-Belt Effects	33
	c. Signal Scintillation Effects	37
V.	CONCLUSION	41
	REFERENCES	43

ACCESSION for	
NTIS	Write Section <input checked="" type="checkbox"/>
DDC	B.M. Section <input type="checkbox"/>
UNANNOUNCED	<input type="checkbox"/>
JUSTIFICATION	
BY	
DISTRIBUTION/AVAILABILITY CODES	
DATE	SPECIAL
<div style="border: 1px solid black; width: 100px; height: 50px; position: relative;"> A </div>	

FIGURES

1.	Argon propellant mass necessary for the transport of different payload masses between 350 km altitude and synchronous altitude	11
2.	Fraction of mission lifetime μ spent at various geocentric distances	13
3.	Number of Ar^+ ions released at various geocentric distances for a payload mass of 10^7 kg, compared to the number of ambient electrons in a dipole field shell two argon gyroradii thick.	14
4.	Energy content versus geocentric distance for the two populations shown in Fig. 3	15
5.	Equatorial loss cone angles (100 km loss cones) for various values of L , calculated for a standard reference geomagnetic field model (after Luhmann and Vampola, 1977)	17
6.	Comparison of charge exchange and coulomb lifetimes of Ar^+ ions at various geocentric distances in the equatorial plane	19
7.	a) Equatorial ion density distributions and b) density distribution along the $L = 4$ dipole field line for the natural plasmasphere model of Chiu et al (1978)	24
8.	Calculated equatorial ion density distributions for various Ar^+ concentrations at the 500 km altitude boundary and several thermal models	25
9.	Field line distributions ($L = 4$) for the models shown in Fig. 8	26

I. INTRODUCTION

The necessity to solve earth-bound socio-economic problems notwithstanding, future directions in space technology may turn towards large-scale utilization, and perhaps colonization, of near-earth space. Indeed, if the concept of collection and transmission-to-earth of solar power in space (power satellite concept) proves feasible, the solution of earth-bound socio-economic problems may actually lie in the full exploitation of space technology. While the economic feasibility of large-scale space systems will not concern us here, we would like to point out that the architectural design of such large-scale systems must take into account not only the efficient functioning of their primary mission objectives, but also their influence upon the operations of other space systems. Since the space environment is tenuous, we find, by analysis of the space transportation requirements, that such large-scale space systems may severely alter the environment in which other space systems operate. To put it more succinctly, the architectural design of large space systems must take into account the interaction among space systems as a major design element.

All large-scale space missions of prolonged duration require transportation of large payloads from low-earth parking orbit, where orbital decay due to atmospheric drag is prevalent, to final orbit where the absence of atmospheric drag permits prolonged operation. Quite obviously, savings of propellant mass for transportation of large payloads from low-earth orbit to final orbit is a primary design consideration since

storage and transportation of propellant mass are at the expense of payload mass. This design element limits the space transportation system to high specific impulse engines which achieve a given propulsion requirement with lower propellant mass by increasing the exhaust velocity. In current technology, such high specific impulses are achieved by acceleration of an ion beam by an electric field, hence the names ion-engine and electric thruster. Small-scale operations of such ion engines in earth and space applications have been effected, although data on large-scale operations are yet to be obtained. While secondary design changes in technology of such ion engines will inevitably occur (some of these will be discussed in Section II), it is perhaps safe to assume at present that some form of beam-plasma engine will be the primary candidate for space transportation of the future. Thus, under very general assumptions, we can pose the following problem: What are the changes of the near-earth space environment induced by injection of very large quantities of propellant ions in the form of beam-plasma exhaust? In this paper, our primary purpose is to raise the systems-designers' awareness of the question rather than to offer complete solutions to the problems which we identified, although such solutions are presently under investigation.

In Section II, a general beam-plasma emission model of space transport systems using electric propulsion is discussed. Thrust parameters characteristic of beam-plasma emissions for the solar power satellite are treated as the nominal example, while parameters for other large-scale missions may be appropriately scaled to the nominal case. In Section III, the major physical interaction of the beam-plasma exhaust with the ambient

magnetospheric-ionospheric plasma and with the Earth's magnetic field is discussed. The comparison and modeled interaction of the exhaust plasma with the natural ambient plasma in the plasmasphere reveals the true magnitude of space environmental modifications induced by such large scale systems. In Section IV, we use the results of Sections II and III to consider the effects upon the operations of other space systems such as interference effects of modified airglow on Earth sensors, modification of radiation belt dosage environment and communication signal scintillation problems due to beam-plasma interactions.

Technically, our consideration raises more questions than it answers; however, it is precisely the raising of such questions which emphasizes that large-scale utilization of space, as well as space colonization, requires that the design include considerations of the interactions between the functions of different space systems.

II. ION EXHAUST EMISSION MODEL

Propulsion requirements of large space systems (Byers and Rawlin, 1976; Stearns, 1976) usually settles on the most economical operation plan of payload boosting into low earth-orbit by chemical rockets and subsequent orbit transfer into deep-space final orbit by the use of high specific impulse ion engines. The impact of chemical propellants upon the atmosphere and lower ionosphere is itself a problem of considerable interest (Mendillo et al., 1975), but it will not concern us here since we shall be concerned exclusively with the ion exhaust.

The ion engine achieves reduction of orbit transfer propellant requirements by ionization and subsequent acceleration by an electric field of the propellant mass in the form of an ion beam. The current technology of ion engines is still evolving (Kauffman, 1974); however, it is by now fairly firm that the most economical and environmentally harmless propellant is argon.

In this paper, we shall assume a nominal argon ion engine operating at an ion temperature of $\sim 1000^\circ \text{K}$ and at a beam current density of $2.5 \times 10^{-2} \text{ Amp/cm}^2$ (Byers and Rawlin, 1976) or $1.6 \times 10^{17} \text{ Ar}^+/\text{cm}^2 \text{ sec}$. The streaming speed of the exhaust beam is $\sim 60 \text{ km/sec}$ for a nominally assumed specific impulse of $\sim 6000 \text{ sec}$. Thus, the ion beam exhaust is a very dense, but fairly cool plasma whose streaming kinetic energy $\sim 500 \text{ eV}$ (corresponding to $\sim 60 \text{ km/sec Ar}^+ \text{ ions}$) far exceeds the thermal energy. Those readers familiar with plasma physics will note that such a plasma in the absence of external devices, as the beam

exhaust will be, is highly unstable since the free streaming energy is available for conversion into thermal or other forms of bound energy. As will be noted in a later section, beam-plasma interactions will be a principal impact; however, the truly staggering scale of that impact can only be appreciated if we consider the total amount of propellants required for such large-scale space systems. Figure 1 shows the relationship between payload mass and argon propellant mass needed to transport the payload from low earth orbit (350 km altitude) to synchronous altitude with an accompanying orbital plane change of 28.5° . Obviously, the amount of propellant required for a given payload depends on the ion-beam streaming speed. For a minimum Solar Power Satellite payload of about 10^7 kg, it will be necessary to expend 10^6 kg of argon propellant (Byers and Rawlin, 1976), which is $\sim 1.5 \times 10^{31}$ Ar^+ ions. By contrast, the total content of the natural plasmasphere and ionosphere above 500 km is $\sim 4 \times 10^{31}$ ions and the entire global content of the ionosphere below 500 km is $\sim 10^{32} - 10^{33}$ ions. As is well known, the densities for the above regions are of the order of $10\text{-}100 \text{ cm}^{-3}$ and are entirely of terrestrial origin. Therefore, the total number of argon ions injected into the ionosphere and plasmasphere during a single nominal large-scale space mission is comparable to the total content of the ionosphere and magnetosphere.

We realize that the above contrast, while staggering, is somewhat misleading because both the time scales of ion injection and the time scales of ion loss are crucial factors in determining the extent of environmental modification. While detailed modelling studies in this area are presently underway, the basic physical processes of the ion emission model can be discussed with some degree of quantification. The exhaust

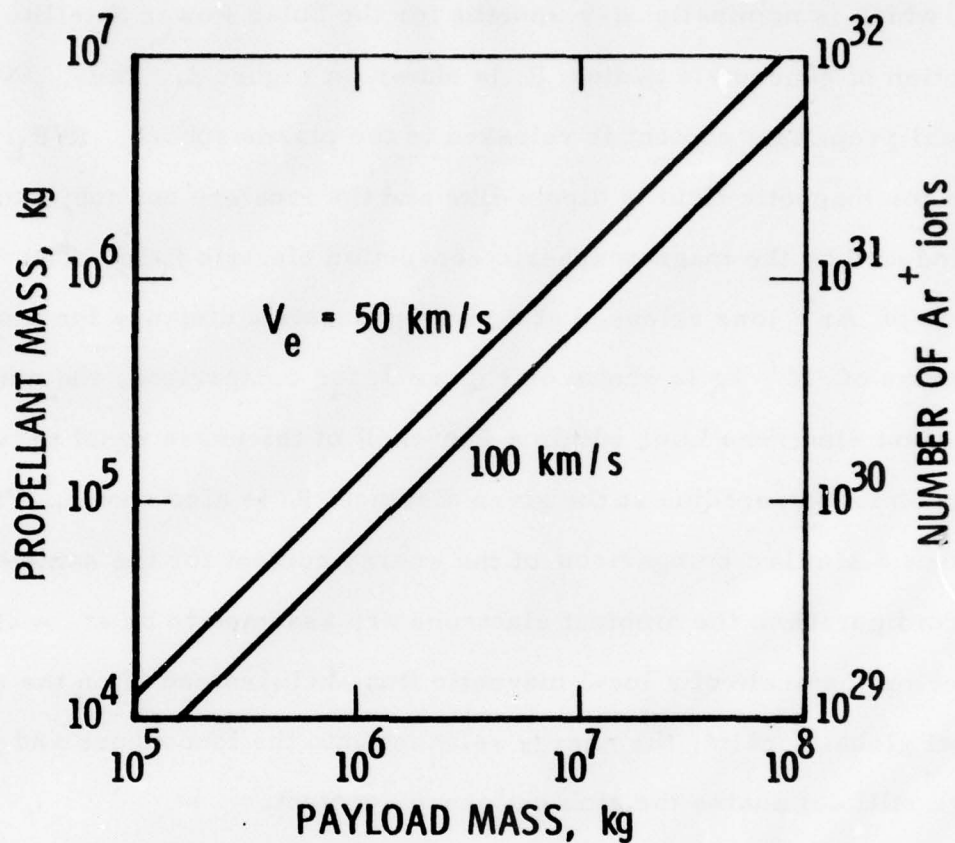


Figure 1 Argon propellant mass necessary for the transport of different payload masses between 350 km altitude and synchronous altitude. The orbital inclination is assumed to change from 0° to 28.5° during transport.

deposition rate in terms of the fraction μ of transportation mission time, which is nominally 6-9 months for the Solar Power Satellite, as a function of geocentric radius R is shown on Figure 2. Thus, 80% of the total propellant content is released in the plasmasphere, $R/R_E \leq 4$, where the magnetic field is dipole-like and the ions are not subject to loss induced by the magnetospheric convection electric field. The number of Ar^+ ions released at a given geocentric distance for a payload mass of 10^7 kg is shown on Figure 3; for comparison, the number of ambient electrons lying within a flux shell of thickness equal to twice the argon ion gyroradius at the given distance R is also shown. Figure 4 shows a similar comparison of the energy content for the same emission configuration; the ambient electrons are assumed to be at $\sim 2000^\circ\text{K}$. Hence, on the scale of a local magnetic flux shell instead of on the scale of total global content, the energy released into the ionosphere and plasmasphere still dominates the ambient energy content.

The comparisons of local, instead of global, injection rates with the contents of the ambient environment presages environmental modification, but it is still not qualitatively conclusive because the loss rates of the injected ions must also be considered. Charged particles in the ionosphere and plasmasphere gyrate about the magnetic field and are not lost to the atmosphere even though they may have a high velocity. They are lost to the magnetosphere if they become neutralized, since neutral particle motion is not confined by the Earth's dipolar magnetic field. The loss of an energetic Ar^+ ion by charge exchange interaction

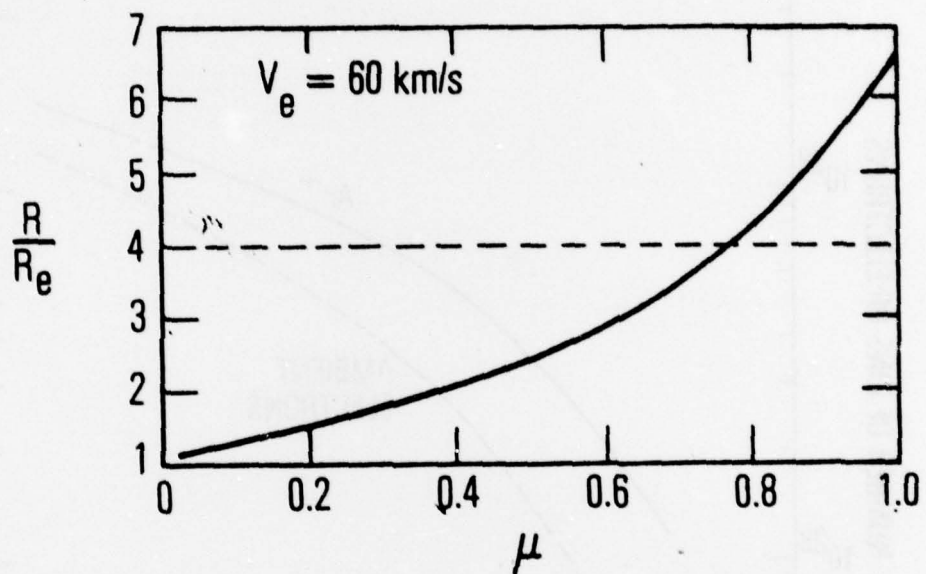


Figure 2 Fraction of mission lifetime μ spent at various geocentric distances.

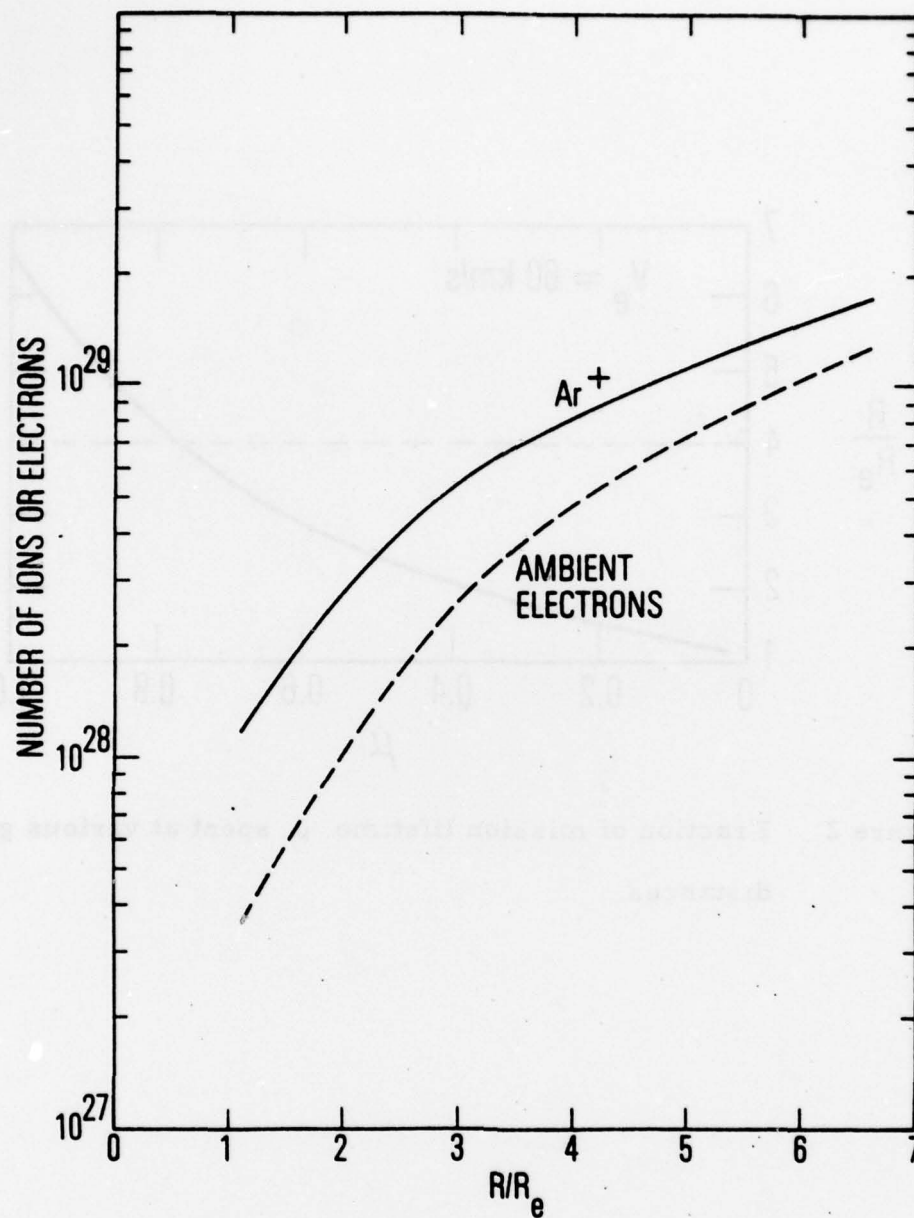


Figure 3 Number of Ar^+ ions released at various geocentric distances for a payload mass of 10^7 kg, compared to the number of ambient electrons in a dipole field shell two argon gyroradii thick.

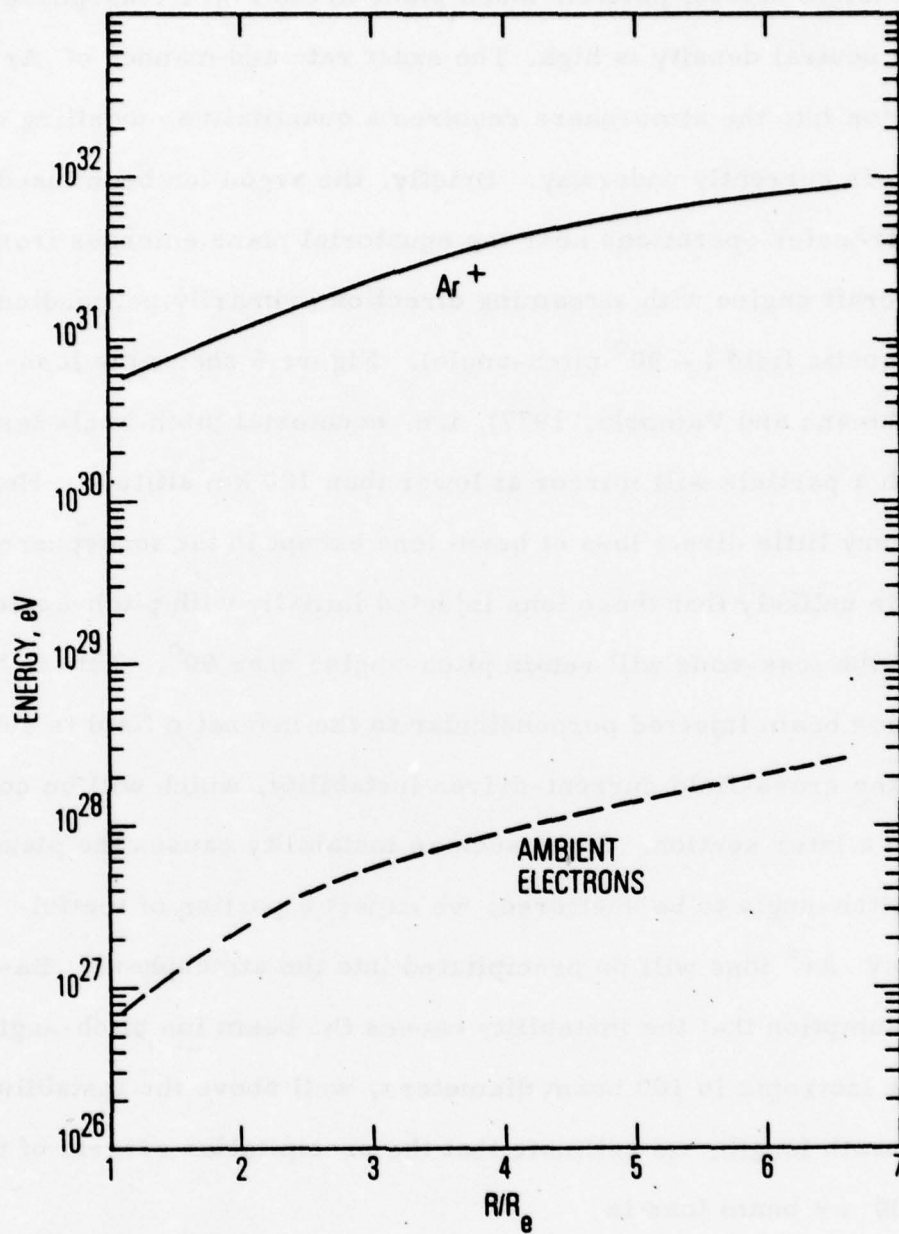


Figure 4 Energy content versus geocentric distance for the two populations shown in Fig. 3.

with an ambient neutral particle takes place in the lower ionosphere where the neutral density is high. The exact rate and manner of Ar^+ precipitation into the atmosphere requires a quantitative modelling effort which is currently underway. Briefly, the argon ion beam used for orbit transfer operations near the equatorial plane emerges from the spacecraft engine with streaming direction primarily perpendicular to the magnetic field ($\sim 90^\circ$ pitch-angle). Figure 5 shows the loss-cone angle (Luhmann and Vampola, 1977), i.e. equatorial pitch-angle less than which a particle will mirror at lower than 100 km altitude. Hence, there is very little direct loss of beam ions except in the ionosphere, although it is unlikely that those ions injected initially with pitch-angles outside of the loss-cone will retain pitch-angles near 90° . This is because an ion beam injected perpendicular to the magnetic field is subjected to the cross-field current-driven instability, which will be considered in a later section. Since such an instability causes the plasma particle pitch-angle to be scattered, we expect a portion of the initial 500 eV Ar^+ ions will be precipitated into the atmosphere. Based on the assumption that the instability causes the beam ion pitch-angles to become isotropic in 100 beam diameters, well above the instability spatial growth length, we estimate that the precipitation current of the initial 500 eV beam ions is

$$J \leq 10^{12} \sin^2 \alpha_L, \text{ Ar}^+/\text{cm}^2 \text{ sec};$$

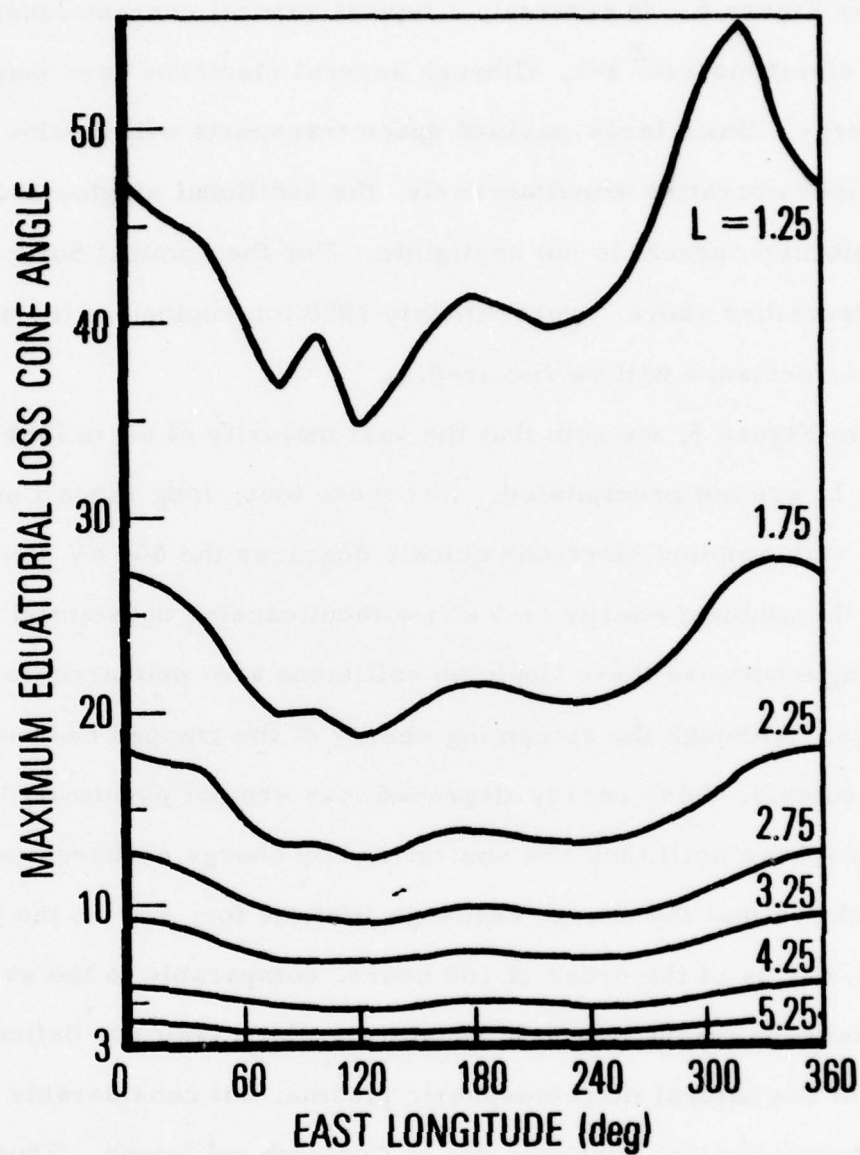


Figure 5 Equatorial loss cone angles (100 km loss cones) for various values of L , calculated for a standard reference geomagnetic field model (after Luhmann and Vampola, 1977).

where α_L is the loss-cone angle at a given equatorial distance $L = R/R_E$, as given by Figure 5. In contrast, a typical auroral current density is $10^8 - 10^9$ electrons/cm² sec, although auroral electrons have somewhat higher energy. Since large-payload space transports will involve thousands of ion engines operating simultaneously, the additional airglow induced by the precipitation current is not negligible. For the nominal Solar Power Satellite described above, approximately 1000 ion engines of the above nominal performance will be required.

From Figure 5, we note that the vast majority of beam ions injected at higher L are not precipitated. For these ions, long range Coulomb collisions with ambient electrons quickly degrades the 500 eV streaming energy to the ambient energy (~ 5 eV) without causing substantial changes in pitch-angle because these Coulomb collisions are primarily forward scatterings. Although the streaming energy of the trapped beam-ions degrades quickly, these energy-degraded ions are not physically lost from the plasmasphere until they are neutralized by charge exchange interaction. Figure 6 shows that the charge exchange lifetime for Ar^+ in the plasmasphere ($L \geq 2$) is of the order of 100 hours, comparable to the average duration between magnetospheric substorms which typically defines the lifetimes of the natural magnetospheric plasma, but considerably longer than the thermalization lifetimes due to Coulomb collisions. Thus, for the duration of the large-scale space mission, the plasmasphere and upper ionosphere is modified by a steady source of Ar^+ ions about equal to the global and local contents of these regions, but the energy content of these regions will increase by one or two orders of magnitude over the natural environment.

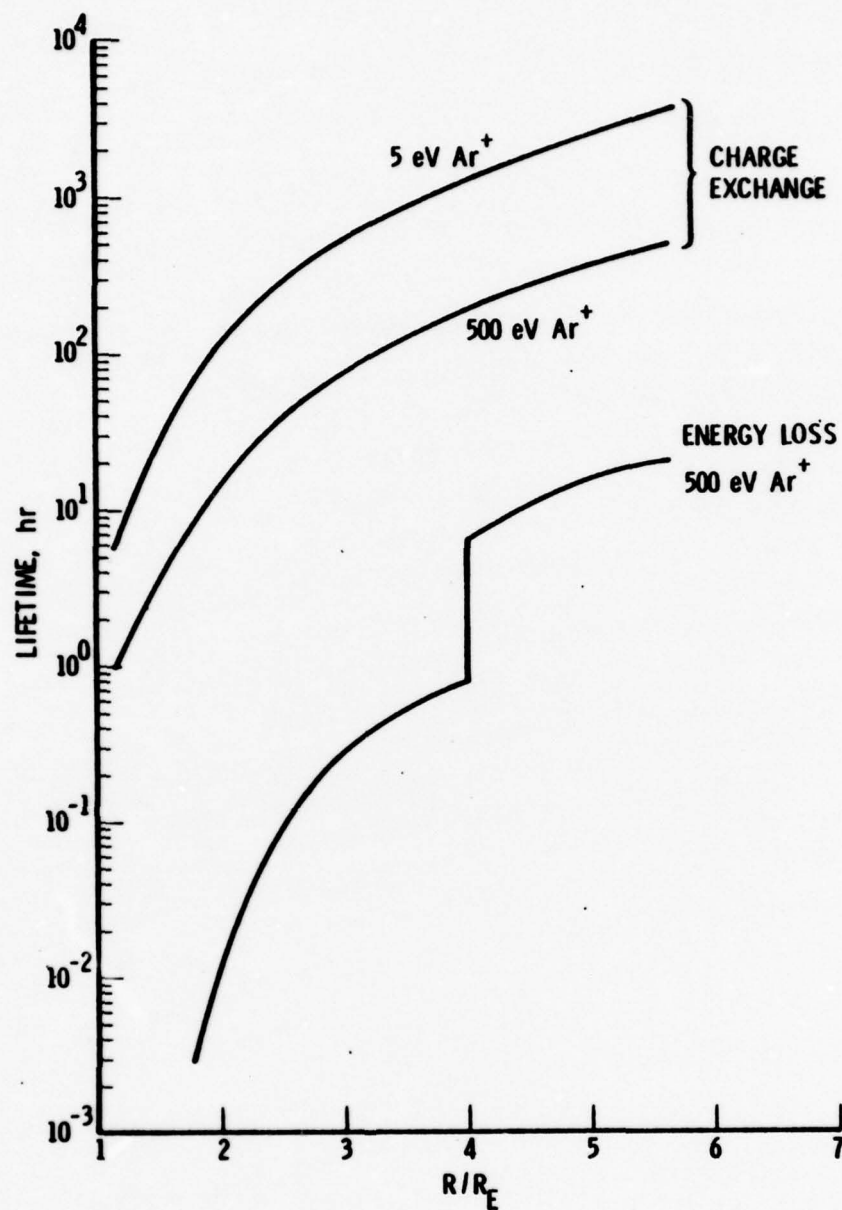


Figure 6 Comparison of charge exchange and coulomb lifetimes of Ar^+ ions at various geocentric distances in the equatorial plane. The charge exchange cross section used in the calculation of the lifetime was measured by Gilbody et al (1965). The plasmopause is assumed to occur at 4 R_E .

III. PLASMASPHERE MODEL WITH ARGON

In an earlier report, Chiu et al. (1978) introduced an equilibrium model of the natural plasmaspheric composition and density in the region bounded by the 500 km altitude level and the dipole field line $L = 5$. This fluid-equation model included the effects of density and compositional distribution due to the gravitational field, the ambipolar diffusion electric field, rotation, and the inhomogeneous dipole magnetic field. The boundary conditions for the model consisted of the density and composition at the 500 km level, and a temperature distribution based on satellite measurements. According to satellite measurements, the temperature distribution of the plasmasphere depends on the magnetic invariant latitude and the distance along a magnetic field line. Using these phenomenological inputs, the model is able to generate plasmaspheric composition and density in agreement with the totality of satellite and ground-based measurements.

In this section, we shall use this model of the natural plasmasphere to assess the effects of injecting large amounts of argon ions into the plasmasphere. We note at the outset that our considerations here use the simpler time-independent equilibrium model described above (Chiu et al., 1978), whereas a thorough investigation must also consider the effects of plasmaspheric modification during the build-up and decay phases as well. For this reason, our results here are not meant to be taken without reservation. Detailed time-dependent studies are currently underway.

The spatial distribution of argon ions at the instant of their expulsion from the orbit-transfer vehicles was discussed in the preceding section. As has been discussed, the ion beam is unstable to an ion acoustic instability when injection is directed perpendicular to the ambient magnetic field (Barrett et al., 1972). It is believed that this instability will introduce a practically isotropic distribution of argon ions into the plasmaspheric flux tubes before thermalization. Because the bulk of the particles will be found outside of the atmospheric loss cone, the fate of these ions initially depends on their interactions with the other plasmasphere constituents. The comparison described in Fig. 6 indicates that the argon ions in the equatorial plane will thermalize by Coulomb collisions on a time-scale much shorter than their time-scale for removal by charge exchange with ambient hydrogen atoms. Consequently, the argon will not escape confinement by the local magnetic field. The important implication of this result is that the heat deposited as kinetic energy of the argon effluent is redistributed among the ambient plasmasphere ions on a time-scale of hours. Thus, the argon ions heat the natural plasmaspheric ions as they come into thermal equilibrium with the ambient population.

In the forementioned model of the natural plasmasphere, Chiu et al., (1978) included the major ionic constituents O^+ , H^+ and He^+ . For the purpose of the present study, the relatively minor constituent He^+ was neglected and a singly ionized argon component was introduced. The amount of Ar^+ at the 500 km boundary was nominally set equal to either the natural concentrations of oxygen or hydrogen. This is strictly a

simplifying assumption based on the observation that the total content of injected argon is approximately equal to the natural plasmaspheric content. To be more precise, we need to improve our model to include time dependence in order to study the behavior of the boundary conditions. The thermal impact of the injection of the 500 eV ions is incorporated into the model by increasing the overall temperature (see equation 2) by factors of 2-8. Thus, the situation under consideration is represented by an equilibrium, heated plasmasphere with a specific argon ion concentration in the ionosphere.

Figure 7 shows both the equatorial ion density distributions and the distributions along the $L = 4$ dipole field line for the natural plasmasphere described by Chiu et al., (1978). The changes resulting from the addition of suprathermal Ar^+ ions are illustrated by Figs. 8 and 9. In Fig. 8 the redistribution of the equatorial densities is shown for several temperature structures and ionospheric concentrations. The corresponding density distributions along the field line $L = 4$ are shown in Fig. 9. Both Fig. 8 and Fig. 9 indicate that the total number density will increase at all altitudes compared to the natural plasmasphere. However, for the natural plasmasphere, H^+ is the dominant ion above ~ 2000 km altitude, while the addition of substantial heat by the Ar^+ ions can drive O^+ into the higher regions of the plasmasphere. The O^+ becomes less earthbound through the combined effect of the scale height increase and the ambipolar diffusion electric field. One is consequently faced with the prospect of evaluating the impact of a heated oxygen plasmasphere containing substantial amounts of Ar^+ at topside ionospheric altitudes.

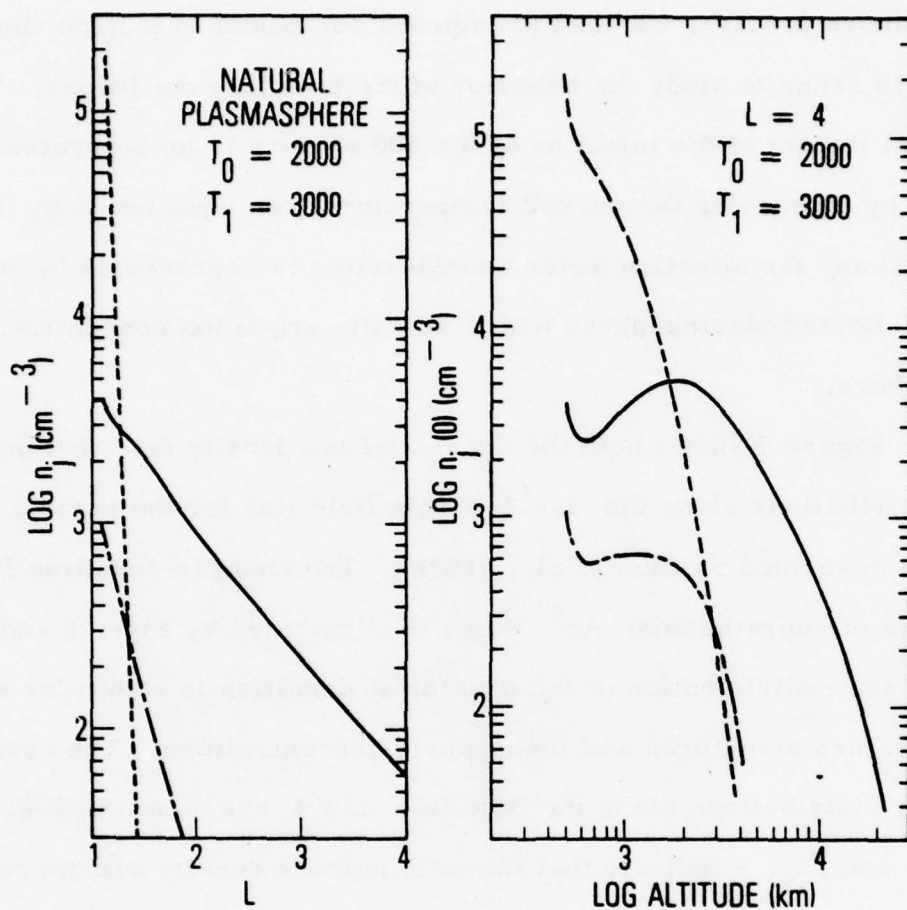


Figure 7 a) Equatorial ion density distributions and b) density distribution along the $L = 4$ dipole field line for the natural plasmasphere model of Chiu et al (1978). In both panels, the dashed curves refer to O^+ , the solid curves refer to H^+ and the curves with long and short dashes refer to He^+ .

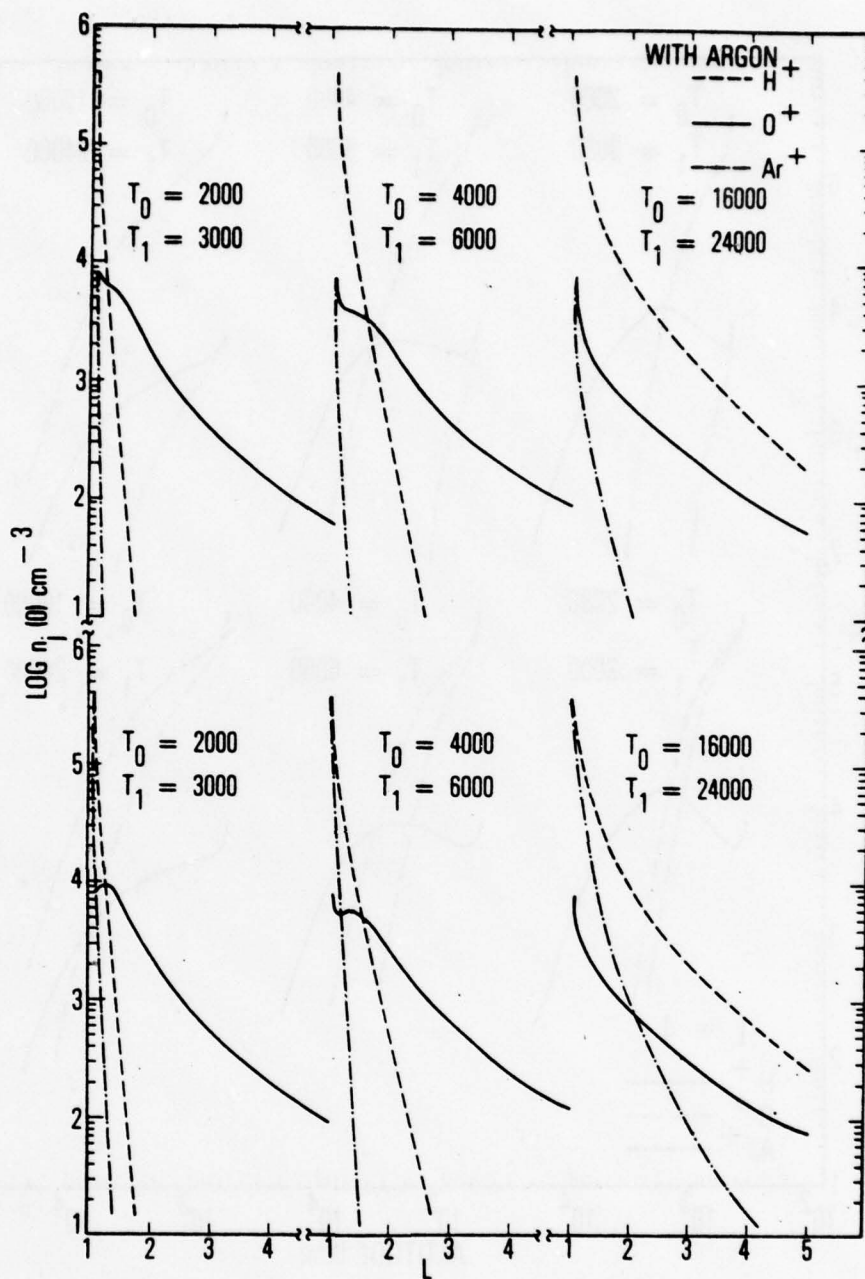


Figure 8 Calculated equatorial ion density distributions for various Ar^+ concentrations at the 500 km altitude boundary and several thermal models.

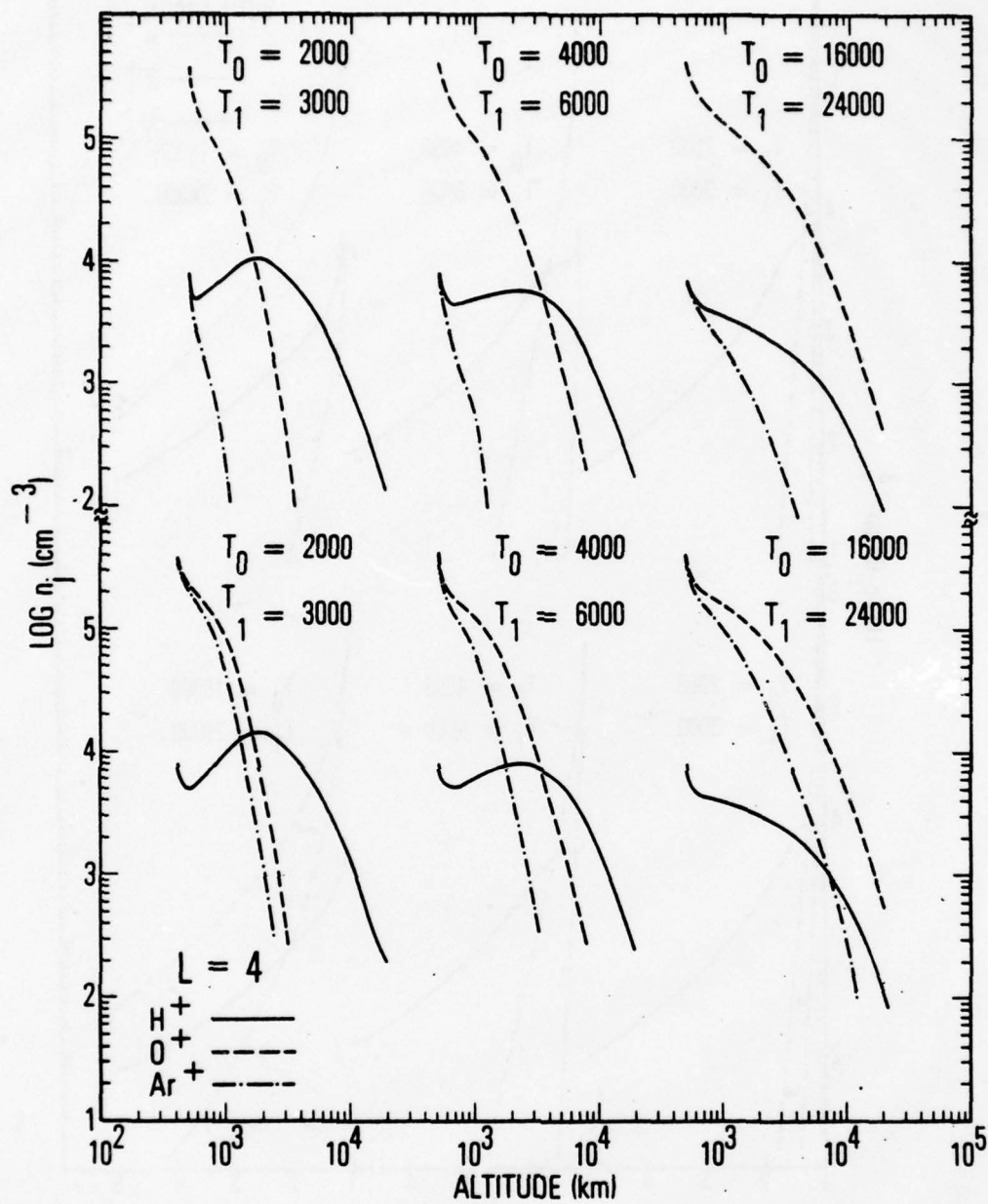


Figure 9 Field line distributions ($L \approx 4$) for the models shown in Fig. 8.

IV. IMPACT ON SPACE SYSTEMS

a. Effects on Atmospheric Optical Sensing Systems

Space-based optical sensors that peer at or through the earth's atmosphere for meteorological, scientific, or earth-resource applications are widely used at the current time, and prognostications indicate even further exploitation of remote sensing techniques in the near future. The interpretation of data from such systems must, of course, take into consideration the optical emissions that emanate from the atmosphere itself, for many if not most applications the atmospheric emissions represent an unavoidable background against which measurements must be made. Quite understandably, any changes in the background would have impact on the performance of such systems via their effect on data analysis and interpretation. In cases of extreme changes in the background it is not inconceivable that sensor design modifications might be required.

In this section we shall explore the possibilities of changes in the emission spectrum of the atmosphere stemming from the introduction of Ar^+ ions into the ionosphere and the concomitant modification of the thermal budget of the ionosphere as described earlier. Basically, we need only consider sub-auroral latitudes since, as discussed previously, the bulk of the ion-engine propellant will be released within the plasmasphere ($L \gtrsim 4$). In addition, we shall confine the discussion to processes that occur at altitudes above about 100 km as it appears

unlikely that ion-engine effluents would have much impact below that height.

In the unperturbed sub-auroral region of the upper atmosphere the optical emissions are called collectively "the airglow," and they range in wavelength from the extreme ultraviolet to the far infrared. These radiations, which are comprised mainly of lines and bands of atomic and molecular oxygen and nitrogen, nitric oxide, and hydrogen, are produced by various processes such as resonant and fluorescent scattering of sunlight, photoelectron excitation, and chemical interaction. It is instructive at this point to distinguish between photoelectrons in the ionosphere, which are the immediate product of the photoionization of neutral atmospheric particles, and the ambient electron gas, which is the ensemble of electrons that have reached thermal equilibrium. Photoelectrons are the more energetic of the two populations, capable even of producing further ionization, whereas the thermal electrons in the present undisturbed ionosphere have energies only of the order of a few tenths of an electron volt.

In the scenario of the ion-engine perturbed ionosphere, the photoelectron energy distribution will be unaffected (since it results from the interaction of solar extreme ultraviolet photons and neutral gas particles), but the mean thermal electron energy will be higher as a result of the thermalization of the 500 eV Ar^+ effluents. In accordance with the previous sections, we shall assume the new equilibrium state to be represented by 5 eV electrons.

Two distinct disturbance phenomena need to be considered: (1) those associated with the transient precipitation of 500 eV argon ions into the upper atmosphere (see Section II), and (2) those associated with the new equilibrium state characterized by 5 eV thermal electrons.

The first case involves a process that is not common in the unperturbed subauroral atmosphere: heavy particle bombardment. Precipitation of heavy particles is usually reserved only for the high-latitude region; even then the particles (protons) are not as massive as argon ions. The precipitation of 500 eV argon ions will produce emissions from the second positive system of N_2 and the first negative system of N_2^+ (Liu and Broida, 1970), both of which lie in the ultraviolet. From the expression for the precipitating Ar^+ flux given in Section II and the variation of the loss cone as a function of L shown in Fig. 5, it is easy to see that the precipitation of Ar^+ will decrease rapidly as the spiraling spacecraft moves to higher and higher L-values. Using the total charge transfer cross section for Ar^+ on N_2 (Hedrick et al., 1977) and the cross section for the reaction leading to N_2 and N_2^+ band emission (Liu and Broida, 1970, and assuming that this cross section does not change significantly between 500 and 900 eV), we calculate that the intensity of the emission ranges from 5 to 0.1 kR (kilorayleighs) for L-values between 1.25 and 4, respectively. For comparison, the normal day glow intensity in these bands is of the order of 1 kR.

Since this first case involves 500 eV argon ions which are precipitated directly from the ion beam before thermalization, a moving region of emission stimulated by precipitating Ar^+ will essentially track the foot of the field line that connects to the spacecraft in the equatorial plane.

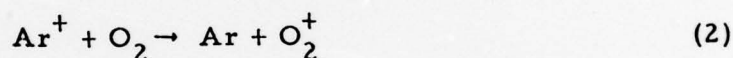
Let us next consider the modifying effects of the new equilibrium state. If the total electron content and its altitude distribution are changed, this will, of course, affect the airglow processes. However, a quantitative description of the results is not possible without a detailed model of the "new" ionosphere. Hence, we shall defer such discussions. We can, however, pursue in general terms the ramifications of the increase in the main thermal electron energy of from ~ 0.2 eV to ~ 5 eV.

The most important consequence appears to be the enhancement of the well-known atomic oxygen lines at 5577 Å and 6300 Å. The ^1S and ^1D states of atomic oxygen, which lie at about 4 and 2 eV, respectively, above the ground state and give rise to the aforementioned lines, can easily be excited by the 5 eV thermal electrons. Under "normal" (present-time) conditions these lines originate from photoelectron impact and ion-chemical processes, the 0.2 eV thermal electrons lacking sufficient energy to create the parent state in atomic oxygen.

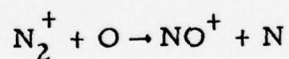
Electronic excitation of N_2 will not be possible since the first level above the ground state requires ~ 6.2 eV for excitation. However, vibrational levels of the ground state can be easily excited, and this may

indirectly affect the airglow phenomenology through the following sequence: (1) vibrationally excited N_2 reacts more readily with O^+ to form NO^+ ; (2) NO^+ dissociatively recombines rapidly with electrons leading to an excited nitrogen atom; (3) the nitrogen atom radiates at 5200\AA .

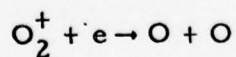
In a similar context, the presence of thermalized argon ions may also modify the airglow intensity because they react efficiently with N_2 and O_2 in charge exchanging processes:



Process (1) is followed by



which is sufficiently exothermic to electronically excite either product. Process (2) is immediately followed by the dissociative recombination reaction



in which one or both of the oxygen atoms may be excited and capable of radiating at either 5577\AA or 6300\AA .

In summary, it is seen that there is great potential for modification of the airglow that may have impact on optical sensor systems. In particular, directly precipitated 500 eV Ar^+ ions stimulate N_2 airglow emissions at a level comparable to the natural level and thermalized 5 eV ambient electrons of the modified ionosphere may greatly enhance atomic oxygen airglow, which under natural circumstances are stimulated by low fluxes of photoelectrons, whose energy spectrum is mainly dominated by electrons with energies below a couple of electron volts. In addition, the energy cascade into the 100 km region may also stimulate increased molecular airglow at infrared frequencies.

b. Ring-Current and Radiation-Belt Effects

The widespread use of ion engines in space carries certain implications for the high-energy ($E \gtrsim 10$ keV) particles that populate the earth's magnetosphere. The effects of ion engines on such high-energy populations are necessarily indirect, since the injected argon ions have energies of at most 500 eV. The high-energy particles, however, are subject to the magnetospheric environment, and the level of such turbulence may possibly be enhanced or reduced by the addition of argon ions from a space engine.

It is customary, for both kinematical and dynamical reasons, to distinguish between particles having $E \sim 10 - 100$ keV and those having $E \gtrsim 100$ keV. The former are known as ring-current particles, since they account for the major share of diamagnetic disturbances observable with low-latitude magnetometers at the earth's surface. The latter are known as radiation-belt particles, since they account for most of the radiation damage to hardened spacecraft. The ring current and the radiation belts consist of electrons, protons, and heavier ions trapped in the earth's magnetic field. Such particles obey the laws of adiabatic charged-particle motion in the first approximation, and their iso-intensity profiles are toroidal in shape (e.g., White, 1966).

The ring current and radiation belts are populated with energetic particles by virtue of the dynamical interaction between the earth's magnetosphere and the solar wind. They are depleted of such particles mainly by interaction with plasma turbulence, which tends to violate the adiabatic

invariants of charged-particle motion. Such violation allows particles to escape confinement by the earth's magnetic mirror and to precipitate (i. e., deposit their energy) in the earth's atmosphere and ionosphere. However, the interaction of geomagnetically trapped particles with plasma turbulence is very selective, in that it is contingent upon a "resonance" between the gyration of a particle and the frequency of a wave in the turbulent spectrum (after one takes account of the Doppler shift associated with the motion of the particle through the plasma). Thus, different classes of turbulence are found to interact with different classes of particles.

Turbulence in a plasma can be created by various mechanisms. For example, the injection of a cold (i. e., mono-energetic) ion beam into a background plasma can easily lead to instability in various electrostatic wave modes (e. g., Hasegawa, 1975). The consequence of such instability is the rapid amplification of thermal noise to appreciable amplitude, such that the beam itself becomes diffused. In the case of ion engine beams, the question is whether the resulting plasma turbulence can interact resonantly with ring-current or radiation-belt particles. The answer to this question is not yet known, since beam-plasma instabilities have not yet been investigated thoroughly in this context.

Another source of instability in the magnetospheric plasma is the velocity-space anisotropy intrinsic to ring-current particle distributions. Since the magnetic mirror points of ring-current protons and electrons are concentrated near the magnetic equator rather than being distributed uniformly along a field line, there must be relatively more energy per degree of freedom

associated with particle gyration than with translation of guiding centers along field lines. This condition can easily lead to instability in certain electromagnetic wave modes. The anisotropy of ring-current electrons can lead to instability of a field-guided wave with right-handed polarization, i. e., the so-called "whistler" wave mode. The anisotropy of ring-current ions can lead to instability of the analogous field-guided wave with left-handed polarization. Both instabilities require the wave frequency to be somewhat smaller than the corresponding particle gyrofrequency. Both instabilities cause velocity-space diffusion so as to reduce the anisotropy of the corresponding charged-particle species, and so as to reduce the lifetime of that species against precipitation into the earth's atmosphere (Kennel and Petschek, 1966; Cornwall, 1966; Cornwall et al., 1970). Moreover, the unstable ion-cyclotron waves generated by the anisotropy of ring-current protons are resonant with relativistic radiation-belt electrons ($E \gtrsim 2$ MeV) and thus account for the observed precipitation of such electrons during the recovery phase of a magnetic storm (Thorne and Kennel, 1971; Vampola, 1971). It happens that the electromagnetic instabilities noted here are not effective at ring-current energies for protons outside the plasmasphere, since the larger phase velocities attained there require a correspondingly larger proton energy for cyclotron resonance. Thus, the precipitation of relativistic electrons is contingent on the spatial co-existence of ring current and plasmasphere, which occurs only during the plasmaspheric expansion characteristic of the recovery phase of a magnetic storm.

The electromagnetic proton-cyclotron instability, however, is likely to be suppressed by the presence of substantial numbers of heavy

ions such as argon in the magnetospheric plasma (Cornwall and Schulz, 1971). This means that the major mechanism for the depletion of relativistic electrons from the outer radiation belt is likely to be made inoperative by the widespread use of ion engines in space. The present population of such penetrating electrons is kept in balance by the occurrence of several large magnetic storms per year. Suppression of the proton-cyclotron instability might, therefore, result in a major enhancement of the radiation level from relativistic electrons within a year after argon-ion saturation of the plasmasphere.

There is no danger that the population of ring-current protons would be similarly enhanced, since these are subject to rapid charge exchange with ambient neutral hydrogen, as are ring-current helium and oxygen ions on a substantially longer time scale (Tinsley, 1976; Lyons and Evans, 1976). Moreover, the addition of argon plasma (or any other type of plasma) to the natural plasmasphere would tend to enhance the loss rate of ring-current electrons (Brice, 1970; 1971). One should not worry about the development of a charge imbalance in the magnetosphere on account of modified precipitation rates. There is ample cold plasma in the plasmasphere to balance charges through minor modifications of the already weak ambipolar electric field, as has been included in the model calculations of the previous section.

c. Signal Scintillation Effects

The equatorial regions of the plasmasphere and ionosphere, out to geosynchronous orbit, are the environment in which satellite communication systems operate. Since modern transionospheric communication and navigation systems tend to use gigahertz frequencies, the steady modifications of the plasmasphere, such as considered above, do not have any marked effect upon these systems if the plasmaspheric modifications do not involve density irregularities. However, readers familiar with plasma physics will realize that it is a virtual impossibility to keep a plasma quiescent. In the present case of the injection of ion-engine beam-plasma exhaust, the occurrence of plasma turbulence is expected since a beam-plasma system is highly unstable (Barrett et al., 1972). Therefore, an inevitable fact-of-life to be recognized by designers of future large-scale space missions is that the plasma emissions of the system may interfere with communication and navigation systems. Since the magnitude of these interference effects is substantial, it is fortunate that the effects are also transient in nature (as far as we have been able to determine); hence we expect that it will be necessary to coordinate operations with various space systems which depend on communication and navigation signals to insure their function at acceptable levels during the large-scale mission lifetime.

The anticipated signal scintillation effects, or equivalently the formation of plasma irregularities connected with ion engine beam-exhaust in the plasmasphere, can be attributed to two distinct classes of phenomena: a) the current-driven plasma instability of the exhaust beam, and b) plasma drift instabilities associated with the density gradients of the exhaust plasma. The former is very intense because the exhaust beam has a great deal of available free streaming energy (~ 500 eV per Ar^+), but the turbulent region will probably be confined to the vicinity of the space transport. The latter includes

a number of individual plasma instabilities which may occur over an extensive region and at a range of natural environmental parameters since the instabilities are associated with the diffusion of the injected plasma cloud.

The cross-field current-driven ion acoustic instability has been observed in beam-plasma devices with operating conditions similar to those projected for ion engines (Barrett et al., 1972), except that the ion engines will have much higher beam current. This instability draws its energy from the free energy of the streaming plasma beam and generates ion acoustic waves (density irregularities) propagating at large angles to the magnetic field. These waves have frequencies well below the electron cyclotron frequency and have wavelengths of the order of the electron gyroradius, which is ~ 30 cm in the ionosphere and is ~ 20 m at $4 R_E$. Since signal scintillation effects are most severe when the signal wavelength closely matches the irregularity size, we expect that the 30 cm irregularities of the beam-plasma instability will cause severe signal scintillation effects at carrier frequencies of ~ 1 GHz. Currently, a number of civilian and military communications and navigation systems operate in this frequency region.

Drift instabilities draw their energies from the free energy available in plasma density gradients and are instrumental in the diffusion of plasma density concentrations. Observational evidences of drift-induced density striations are available from numerous plasma injections in the magnetosphere ranging from barium releases to nuclear detonations at high altitude. Since these instabilities are not directly related to the beam-exhaust, but are related to the plasma cloud after the streaming plasma beam motion has been randomized, we would expect that rather large areas will be striated. Further, since there is a virtual zoo of drift related instabilities, including those induced by interaction with the neutral wind, the scale sizes of the density

irregularities will probably be broadband; although, if the natural equatorial spread-F condition is any guide, drift-induced density irregularities will probably affect VHF and UHF more severely than frequencies in the gigahertz range.

V. CONCLUSION AND DISCUSSION

Future large-scale space missions, such as the proposed Solar Power Satellite and Space Colonization, will probably require deep-space transportation systems based on the high specific-impulse ion engine. We note in this paper that the ion exhaust emissions corresponding to the proposed large payloads required for such missions will introduce basic modifications in the composition and dynamics of the ionosphere and magnetosphere. We identify some effects that such modifications may induce upon other space systems such as earth sensors, radiation belt dosage environment and signal scintillation due to beam-plasma interactions. We find that, because the space environment is tenuous, there is an interaction among such large-scale space systems and other earth-oriented space systems. The architectural design of such large-scale systems must take into account not only the efficient functioning of their primary mission objectives, but also in terms of their influence upon the operations of other space systems.

The nominal Solar Power Satellite orbit transfer mission discussed in our paper assumes present state-of-the-art ion engines whose characteristics are summarized in Section II. However, since such missions may not take place until the beginning of the 21st century, we expect that significant advances in the technology of ion engines may change the situation somewhat. For example, if the specific impulse of the ion engines is increased by say an order of magnitude, then the total amount of Ar^+ ion exhaust will be reduced by an order of magnitude; however,

the energy of the Ar^+ ions will correspondingly be increased (as the square of the specific impulse) to the order of 10 keV. The presence of such energetic ions introduce entirely new effects upon the radiation belt particles since the bulk of ions in the magnetic storm ring current is in such an energy range. As a further example, it is possible that a hybrid chemical (LO_2/LH_2) and ion engine propulsion scheme may be used to speed up the transfer from low earth orbit to geosynchronous orbit. Such a scheme may also reduce Ar^+ emissions but a new problem of neutral oxygen injection into the magnetosphere will be raised. We have not considered these alternatives, but we hope that the necessity to consider the interaction among space systems operating in the magnetosphere may become integral elements in the consideration of these alternatives.

REFERENCES

- Barrett, P. J., B. D. Fried, C. F. Kennel, J. M. Sellen and R. J. Taylor, Cross-field current-driven ion acoustic instability, Phys. Rev. Letters, 28, 337, 1972.
- Brice, N., Artificial enhancement of energetic particle precipitation through cold plasma injection: A technique for seeding substorms?, J. Geophys. Res., 75, 4890, 1970.
- Brice, N., Harnessing the energy in the radiation belts, J. Geophys. Res., 76, 4698, 1971.
- Byers, D. C. and V. K. Rawlin, Electron bombardment propulsion system characteristics for large space systems, Twelfth International Electric Propulsion Conference, American Institute of Aeronautics and Astronautics, Key Biscayne, Fla., Nov. 15-17, 1976.
- Chiu, Y. T., J. G. Luhmann, B. K. Ching and D. J. Boucher, Jr, An equilibrium model of plasmaspheric composition and density, to be published, J. Geophys. Res., 1978.
- Cornwall, J. M., Micropulsations and the outer radiation zone, J. Geophys. Res., 71, 2185, 1966.

- Cornwall, J. M., F. V. Coroniti, and R. M. Thorne, Turbulent loss of ring current protons, J. Geophys. Res., 75, 4699, 1970.
- Cornwall, J. M., and M. Schulz, Electromagnetic ion-cyclotron instabilities in multicomponent magnetospheric plasmas, J. Geophys. Res., 76, 7791, 1971; Correction, J. Geophys. Res., 78, 6830, 1973.
- Gilbody, H. B., and J. B. Hasted, Anomalies in adiabatic interpretation of charge transfer collisions, Proc. Roy. Soc., Ser. A, 238, 1956.
- Hasegawa, A., Plasma Instabilities and Nonlinear Effects, pp. 28-43, Springer, Heidelberg, 1975.
- Hendrick, A. F., T. F. Moran, K. J. McCann, and M. R. Flannery, charge transfer cross sections in argon ion-diatomic molecule collisions, J. Chem. Phys., 66, 24, 1977.
- Kauffman, H. R., Technology of electron-bombardment ion thrusters, Advances in Electronics and Electron Physics, vol. 36, ed. L. Marton, Academic Press, New York, 1974.
- Kennel, C. F., and H. E. Petschek, Limit on stably trapped particle fluxes, J. Geophys. Res., 71, 1, 1966.
- Liu, C. and H. P. Broida, Optical spectra observed during ion-molecule collisions using low-energy N_2^+ and Ar^+ beams, Phys. Rev., 2A, 1824, 1970.

- Luhmann, J.G., and A.L. Vampola, Effects of localized sources on quiet time plasmasphere electron precipitation, J. Geophys. Res., 82, 2671, 1977.
- Lyons, L.R., and D.S. Evans, The inconsistency between proton charge exchange and the observed ring current decay, J. Geophys. Res., 81, 6197, 1976.
- Mendillo, M., G.S. Hawkins and J.A. Klobuchar, A sudden vanishing of the ionospheric F region due to the launch of Skylab, J. Geophys. Res., 80, 2217, 1975.
- Stearns, J.W., Large-payload earth-orbit transportation with electric propulsion, Jet Propulsion Laboratory Technical Memorandum 33-793, September 15, 1976.
- Thorne, R.M., and C.F. Kennel, Relativistic electron precipitation during magnetic storm main phase, J. Geophys. Res., 76, 4446, 1971.
- Tinsley, B.A., Evidence that the recovery phase ring current consists of helium ions, J. Geophys. Res., 81, 6193, 1973.
- Vampola, A.L., Electron pitch angle scattering in the outer zone during magnetically disturbed times, J. Geophys. Res., 76, 4685, 1971.
- White, R.S., The earth's radiation belts, Phys. Today, 19 (10), 00, October 1966.

THE IVAN A. GETTING LABORATORIES

The Laboratory Operations of The Aerospace Corporation is conducting experimental and theoretical investigations necessary for the evaluation and application of scientific advances to new military concepts and systems. Versatility and flexibility have been developed to a high degree by the laboratory personnel in dealing with the many problems encountered in the nation's rapidly developing space and missile systems. Expertise in the latest scientific developments is vital to the accomplishment of tasks related to these problems. The laboratories that contribute to this research are:

Aerophysics Laboratory: Launch and reentry aerodynamics, heat transfer, reentry physics, chemical kinetics, structural mechanics, flight dynamics, atmospheric pollution, and high-power gas lasers.

Chemistry and Physics Laboratory: Atmospheric reactions and atmospheric optics, chemical reactions in polluted atmospheres, chemical reactions of excited species in rocket plumes, chemical thermodynamics, plasma and laser-induced reactions, laser chemistry, propulsion chemistry, space vacuum and radiation effects on materials, lubrication and surface phenomena, photo-sensitive materials and sensors, high precision laser ranging, and the application of physics and chemistry to problems of law enforcement and biomedicine.

Electronics Research Laboratory: Electromagnetic theory, devices, and propagation phenomena, including plasma electromagnetics; quantum electronics, lasers, and electro-optics; communication sciences, applied electronics, semiconducting, superconducting, and crystal device physics, optical and acoustical imaging; atmospheric pollution; millimeter wave and far-infrared technology.

Materials Sciences Laboratory: Development of new materials; metal matrix composites and new forms of carbon; test and evaluation of graphite and ceramics in reentry; spacecraft materials and electronic components in nuclear weapons environment; application of fracture mechanics to stress corrosion and fatigue-induced fractures in structural metals.

Space Sciences Laboratory: Atmospheric and ionospheric physics, radiation from the atmosphere, density and composition of the atmosphere, aurorae and airglow; magnetospheric physics, cosmic rays, generation and propagation of plasma waves in the magnetosphere; solar physics, studies of solar magnetic fields; space astronomy, x-ray astronomy; the effects of nuclear explosions, magnetic storms, and solar activity on the earth's atmosphere, ionosphere, and magnetosphere; the effects of optical, electromagnetic, and particulate radiations in space on space systems.

THE AEROSPACE CORPORATION
El Segundo, California